Cyclic voltammetric behaviour of polyfuran perchlorate doped films

M.J. GONZÁLEZ-TEJERA[1]* and I. CARRILLO[2]

[1]*Dpto. Química Física I, Facultad de Ciencias Químicas, Universidad Complutense, 28040 Madrid, Spain*
[2]*Dpto. Química Industrial y Polímeros, E.U.I.T. Industrial, Universidad Politécnica de Madrid, C/. Ronda de Valencia 3, 28012 Madrid, Spain*
(*author for correspondence, fax: +34 91 3944135, e-mail: mjgonte@quim.ucm.es)

Abstract

Electroactivity with continuous cycling and the electrochemical behaviour of polyfuran perchlorate films (PFu/ClO$_4$) were investigated to determine the reversibility of doping/dedoping processes and the electrochemical mechanism of these processes as a function of the electropolymerization potential. A surface capacitive oxidation mechanism and a diffusion controlled mechanism in the dedoping process were detected when the potential scan rate was varied in D′ films (η_p = 2.3 V). Moreover, D films (η_p = 2.1 V) showed a mixture of mechanism in the reduction processes. The polymeric material was found to deteriorate with continuous charge–discharge over successive days.

1. Introduction

Our interest in conducting polymers led us to investigate the electrochemical behaviour of polymer potentiostatically formed from a heterocyclic monomer such as furan [1]. The synthesis parameters generally have a considerable influence on the electroactivity and morphology of conducting polymers [2–4].

There has been little research published on polyfuran; however, some publications have established the chemical and electrochemical conditions necessary to optimize the synthesis of this polymer [1–3, 5]. In this last paper, Demirboğa et al. studied the effect of temperature on the polymerization rate, which increased as temperature increased. In order to improve the electropolymerization process, Glenis et al. [6] chose terfuran as the monomer because its oxidation potential is considerably lower. They found that its electrochemical and physical properties were strongly dependent on the nature of the electrolyte used during synthesis.

We report the potentiostatic synthesis and cyclic voltammetric behaviour of perchlorate doped polyfuran films (PFu/ClO$_4$) under specific concentration conditions when two different potential values were applied. The deposition potential strongly influences the structure and properties of conjugated polymer as various FTIR studies have demonstrated [7, 8]. Similarly, this parameter influences the production of another conducting polymer such us polypyrrole [9]. In this last article Otero et al. studied the dependence on the polarization potential of current efficiency and the charge storage ability of polypyrrole films obtained in aqueous media. They found that the polymerization efficiency diminished in all potential ranges from 0.8 to 3.2 V vs SCE and that the charge-storage efficiency reached a minimum at 2.0 V. Kaplin et al. [10] investigated the effect of polymerization potential with different electrolytes such as perchlorate solution or toluene sulphonate solution. Their results confirmed that the electrochemical properties and structure of polypyrrole depended on both parameters.

Here, we analysed electroactivity as a function of the sweep rate (v), positive and negative potential limit (E_f and E_i, respectively) and cycling.

2. Experimental details

PFu/ClO$_4$ films were synthesized potentiostatically at two different constant electropolymerization potentials, η_p = 2.1 V (D films) and 2.3 V (D′ films). The electropolymerization time was t_p = 200 s. Furan (Aldrich Chemie, 99%) was vacuum distilled before use in each experiment. The non aqueous electrolyte medium was acetonitrile (MeCN, Carlo Erba, RPE quality) dried over Merck 3Å molecular sieves (0.05% water content [11]) and sodium perchlorate (NaClO$_4$, Aldrich Chemie, 99%). Monomer and electrolyte concentrations were 0.4 and 0.2 M, respectively.

Electrochemical experiments were performed using a Wenking 68FR 0.5 potentiostat with a Wenking VS G72 triangular wave generator connected to a Sefram X-Y

type Yt-25 recorder, and a glass electrochemical cell with one compartment and three electrodes under nitrogen atmosphere. Working and counter electrodes were Pt sheets of 2.4 and 8.0 cm^2, respectively. All potentials were reported with respect to the saturated calomel reference electrode (SCE), which was connected to the cell by a Luggin capillary. The solutions were flushed with nitrogen before synthesis (15 min) and this atmosphere was maintained above the solution at room temperature throughout.

Before each electropolymerization the working electrode was polished with alumina and diamond paste, cleaned in acetone in an ultrasonic bath, washed in hot concentrated sulphuric acid, and finally rinsed copiously with Milli-Q water.

3. Results and discussion

Figure 1 shows the synthesis chronoamperograms of D and D$'$ films. The charges consumed during the electropolymerization processes, Q_p, present a linear relationship with electropolymerization time, t_p, see Figure 2. The rates of charge consumption ($\Delta Q_p/\Delta t_p$) up to $t_p = 5$ s were 114.7 ± 1.2 and 160.8 ± 2.4 for D and D$'$ films, respectively. The linear relationship was maintained from $t_p > 5$ s, although these slopes were lower. These changes of slope confirm a change in the nucleation mechanisms of the polymeric phase [12]. The films were black, homogeneous and adherent to the electrode.

Characteristic cyclicvoltammograms (CVs) of these films and of a bare Pt electrode are shown in Figure 3. These curves were recorded at a potential scan rate of 30 mV s^{-1} using a different cell from that used in the synthesis with the same non aqueous electrolyte without
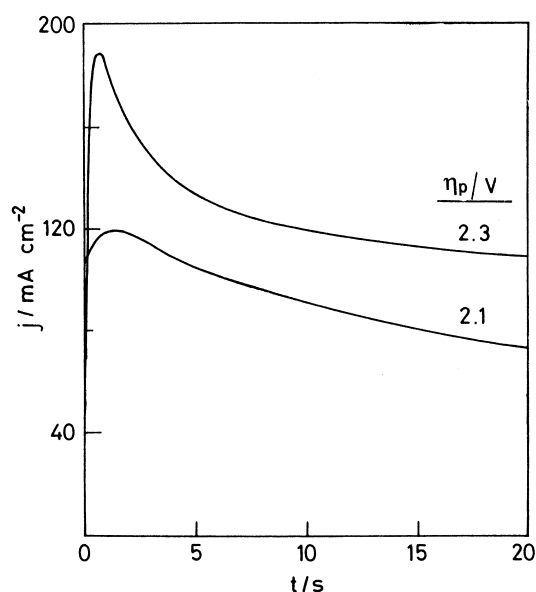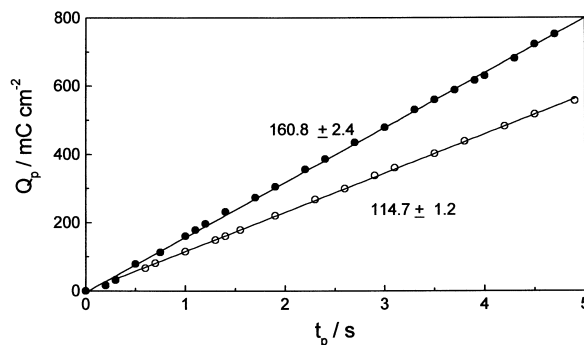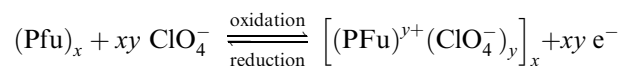
Fig. 2. Plot of polymerization charge density (Q_p) against electropolymerization time (t_p). (○) D films, (●) D$'$ films.

monomer. The first CVs of polymeric deposits showed an anodic wave, **a**, and cathodic waves **a$'$**, **b$'$** and **c$'$** corresponding to different reduction processes of the polaronic states generated through the anodic cycle. In both films, the total oxidation charge (Q_{ox}) was higher than the reduction charge (Q_r) and the ratio between them was near to one.

Electrochemical study of these PFu/ClO$_4$ deposits (D and D$'$) was focused on their behaviour: (a) varying the anodic limit of the CVs (E_f) at constant E_i, (b) varying E_i at constant E_f and (c) at different potential scan rates (v). The effects of continuous cycling were also analysed.

Cyclicvoltammograms recorded from a constant potential $E_i = -1.4$ V to a variable positive value, E_f, from -0.4 to 2.3 V for D film are shown in Figure 4. The aim of these experiments was to generate polaron-type electronic defects in the polymer chain at low positive potentials, and bipolaronic-type defects at higher potentials, since the onset of degradation could take place at these values. The degradation process is connected to anodic overoxidation and is facilitated by the water present in the solvent. These states can produce counterion insertion in the polymeric matrix, which is represented by different peaks or waves in the cathodic cycle. In this semicycle, the deinsertion of dopant anions takes place, as shown in the scheme below:

$$(\text{Pfu})_x + xy\,\text{ClO}_4^- \underset{\text{reduction}}{\overset{\text{oxidation}}{\rightleftarrows}} \left[(\text{PFu})^{y+}(\text{ClO}_4^-)_y \right]_x + xy\,\text{e}^-$$

When the polaronic state (wave **a**) was half formed, $E_f = -0.4$ V, it had a wide reduction wave (**a$'$**). But when it was complete, $E_f = 0.2$ V, the cathodic semicycle in this potential region began to divide into two waves, **a$'$** and **b$'$** (see Figure 4). These reduction waves became more defined as E_f increased. At $E_f \geqslant 1.7$ V, a new reduction wave **c$'$** appeared, indicating the generation of other, bipolaronic oxidation states in the film. The same behaviour was observed in D$'$ films, but a **b$'$** wave appeared when $E_f = 0.6$ V; in other words, dopant insertion was stronger in these films.

The total reduction charge Q_r^T was larger than the oxidation charge Q_{ox}^T until $E_f < 1.7$ V as shown in the insert of Figure 4. Both evolved to the same value when
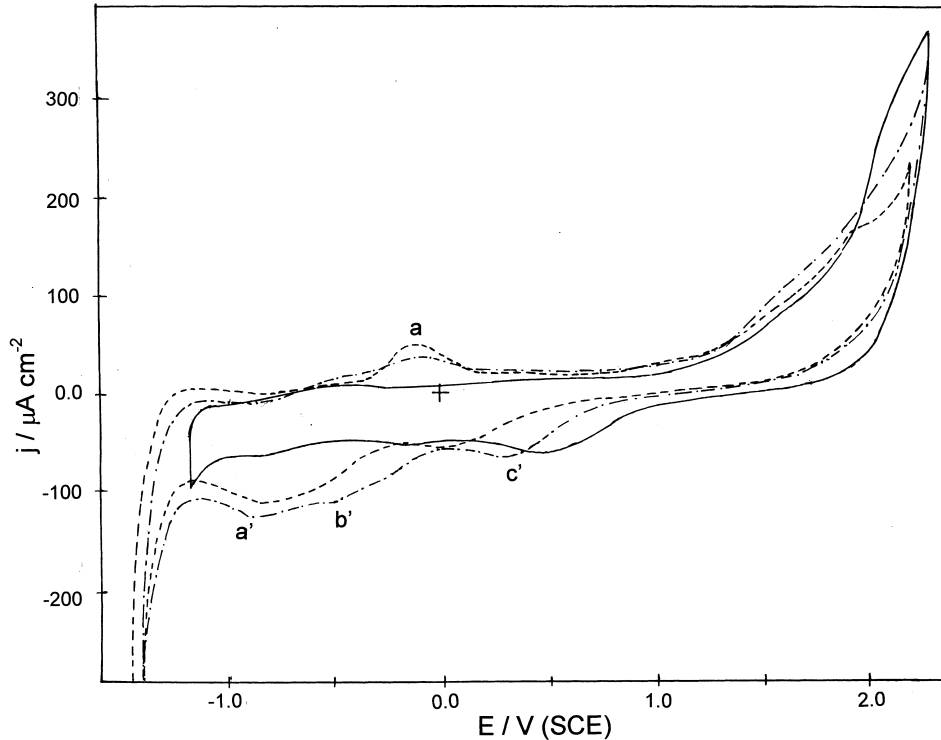
Fig. 1. Chronoamperograms of PFu/ClO$_4$ obtained at $\eta_p = 2.1$ V (D film) and 2.3 V (D$'$ films) (SCE) in [Fu] = 0.4 M and [NaClO$_4$] = 0.2 M.

Fig. 3. CVs of black D (—·—·—), D′ (- - - -) PFu/ClO₄ films and a bare Pt electrode (——) in 0.2 M NaClO₄ + MeCN. Potential scan rate, $v = 30$ mV s⁻¹.
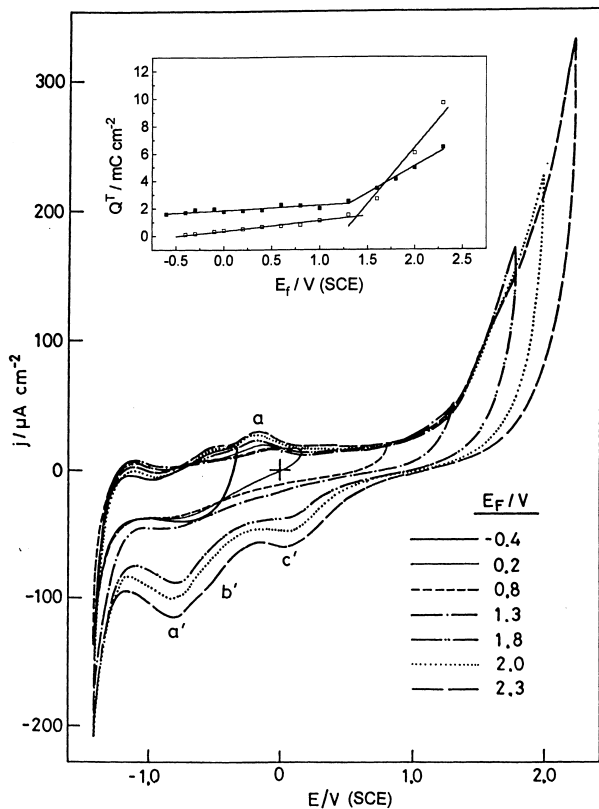

Fig. 4. CVs of **D** films with increasing positive potential limit (E_f) in 0.2 M NaClO₄ + MeCN. $E_i = -1.4$ V. Potential scan rate, $v = 30$ mV s⁻¹. Insert total charge density of oxidation (□) and reduction (■) against positive limit potential.

$E_f = 1.7$ V. Thereafter, Q_r^T was lower than Q_{ox}^T. The ratio Q_r^T/Q_{ox}^T was 0.82 and 0.66 at $E_f = 2.0$ and 2.3 V, respectively. These sub-unity values indicate a deep oxidation level, which signifies considerable counterion penetration and an irregular deinsertion process. Probably the doping and dedoping mechanism changed at $E_f \geqslant 1.3$ V, since at this potential there was a significant change in both Q^T values. To corroborate this fact, the charge density of each wave: **a**, **a′**, **b′** and **c′** was plotted versus E_f (Figure 5). In the range $1.0 < E_f < 1.38$ V, all reduction waves presented a significant slope change, but there were no changes in the oxidation wave (**a**). Similarly, in **D′** films $Q_r^T > Q_{ox}^T$, and these charge densities tended to have a similar value when $E_f = 2.3$ V. The greater oxidation in these films implied a delay in the reversibility of insertion/deinsertion

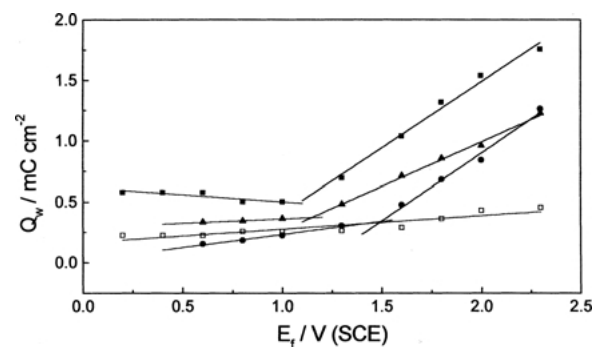*Fig. 5.* Charge density of oxidation wave, **a** (□) and reduction waves **a′** (■), **b′** (▲) and **c′** (●) against positive limit potential (E_f) for D film.
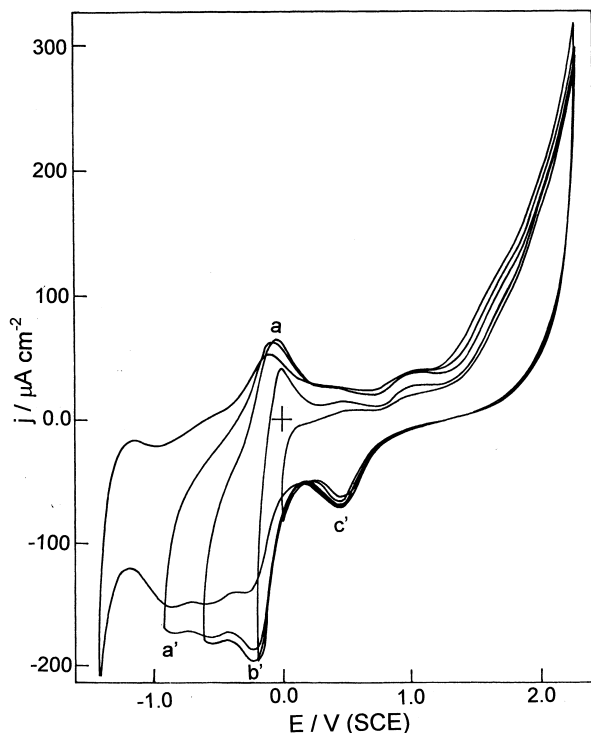
Fig. 6. CVs of D films with increasing negative potential limit (E_i) in 0.2 M NaClO$_4$ + MeCN. Potential scan rate, $v = 30$ mV s^{-1}. $E_f = 2.3$ V.

processes, so that both Q^T values changed at a more positive value of E_f (1.52 V) as in the case of D films. When we evaluated the charge density of each wave in D′ films, a similar slope change was obtained when plotting $Q_{a'}$, $Q_{b'}$, $Q_{c'}$ and Q_a as a function of E_f, but this change occurred over a wider potential range, from 0.75 to 1.52 V. No change was observed in the **a** wave.

To check if PFu/ClO$_4$ films could reach an important degree of dedoping near to the insulating state the negative potential limit was moved from 0.0 to −1.4 V maintaining E_f constant (Figure 6). These experiments were based on the premise that, at negative potentials, the charge carrier density in the films is reduced to practically zero due to positive charges on the polymer being neutralized and counterions being expelled from the polymer. If the Q_r/Q_{ox} ratio reaches one, D and D′ films will be in the insulating state at this specific E_i value. Q_r/Q_{ox} was 0.95, 1.09 and 1.07 when E_i was −0.92, −1.22 and −1.4 V, respectively, in the case of D films and 0.89, 0.93 and 1.14 when E_i was −0.46, −0.63 and −0.78 V, respectively, for D′ films. Dopant anions were more mobile in D′ films in this potential range. When E_i increased in the negative direction, from −0.93 to −1.46 V, the Q_r/Q_{ox} ratio had a constant value equal to 1.3, and so a more reduction state was attained. In both deposits the potential value of oxidation wave **a**
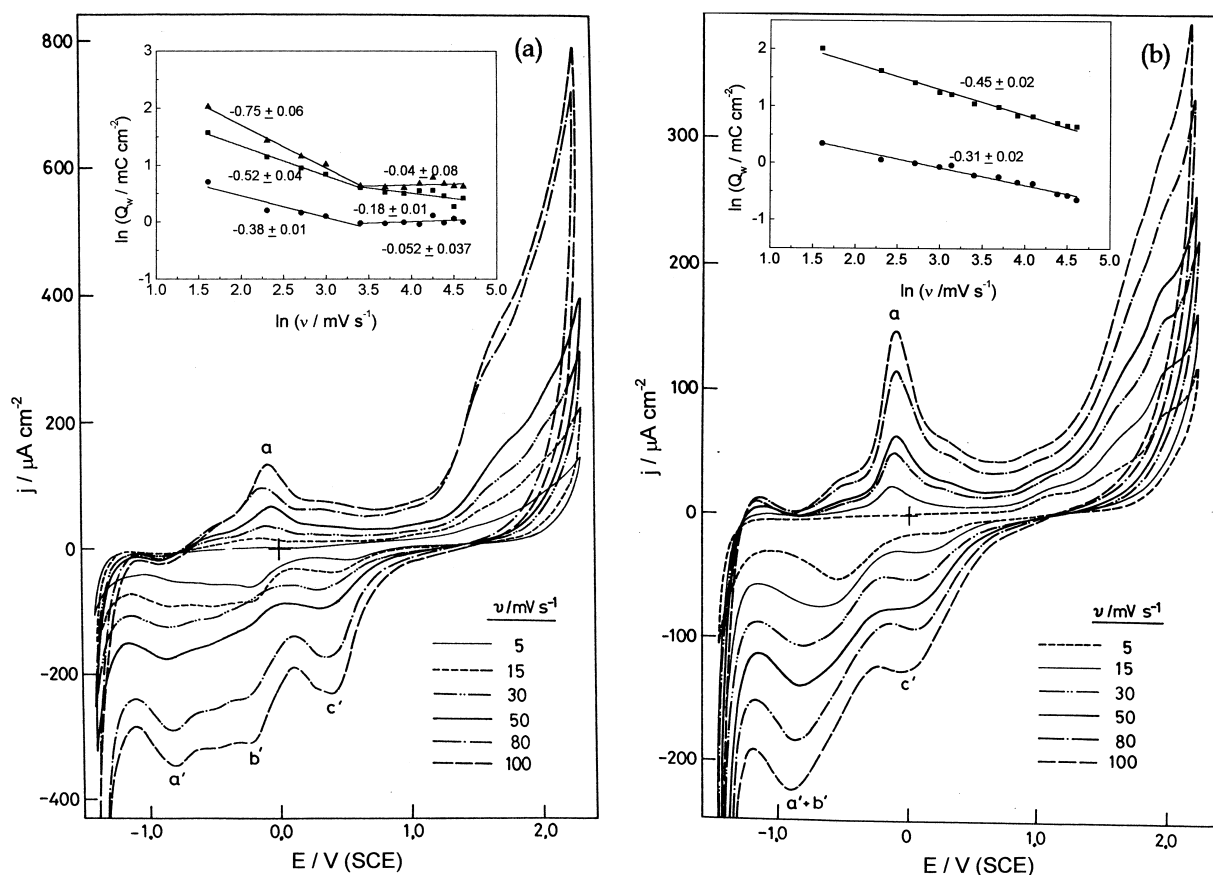

Fig. 7. CVs of PFu/ClO$_4$ films with different potential scan rates in 0.2 M NaClO$_4$ + MeCN. (a) D films, (b) D′ films. Insert logarithmic plot of the charge density of each reduction wave (Q_w) against potential scan rate (v). (a) D films, waves: **a′** (■), **b′** (▲) and **c′** (●); (b) D′ films, waves: **a′ + b′** (■) and **c′** (●).

had a slight deviation when E_i increased negatively, but the potential of the reduction waves remained constant. This could signify reversible permeability of dopant anions, which may be applied in successive charge–discharge cycles for technological applications. It is evident that slow conformational changes in the solid matrix are necessary to open the closed macromolecular entanglement, allowing the entrance of counterions during further oxidation.

The influence of the potential scan rate v in the range 5–100 mV s^{-1} is shown in Figure 7(a) (D films) and 7(b) (D' films). The shapes of these curves are very similar with the exception of the cathodic cycle of D' films where a' and b' waves overlap, probably due to a deep dopant deinsertion process created by the more oxidative state of this deposit. This deduction is also confirmed by the higher values of current densities of a waves in D' films and by the values of the charge density of the a' wave in D film and the $a' + b'$ wave in D' films evaluated as a function of v (see inserts in Figure 7). According to the theory of triangular potential sweep, these slope values establish whether the irreversible electrodic process is mass transfer controlled (diffusion mechanism, slope 0.5), or charge transfer controlled (slope 1.0). The slope of the a' wave up to $v = 30$ mV s^{-1} (D films) and the $a' + b'$ wave for the full range of v indicate whether there is a dedoping diffusive process [13] or a mixture of dedoping mechanisms with different degrees of contribution to the diffusion process. This means that the diffusion mechanism of the dopant anions was prevalent throughout the redox process.

On the other hand, in D films plots of total oxidation and reduction charge densities as a function of potential sweep rate up to $v = 50$ mV s^{-1} showed slopes of -0.48 ± 0.04 and -0.57 ± 0.04 for Q_{ox}^T and Q_r^T, respectively. At $v > 50$ mV s^{-1} the polymer had to have a similar structure because the doping and dedoping charge densities were almost equal. In D' films both slopes had a value of 0.50 ± 0.02.

The wave current densities, j_w, of a, a', b' and c' waves for D films and a, $a' + b'$ and c' waves for D' films as a function of potential scan rate are depicted in Figure 8 according to cyclic voltammetry theory [14–16]. In both films the slope of the a wave was close to unity, indicating that, at this potential, the radical cations were

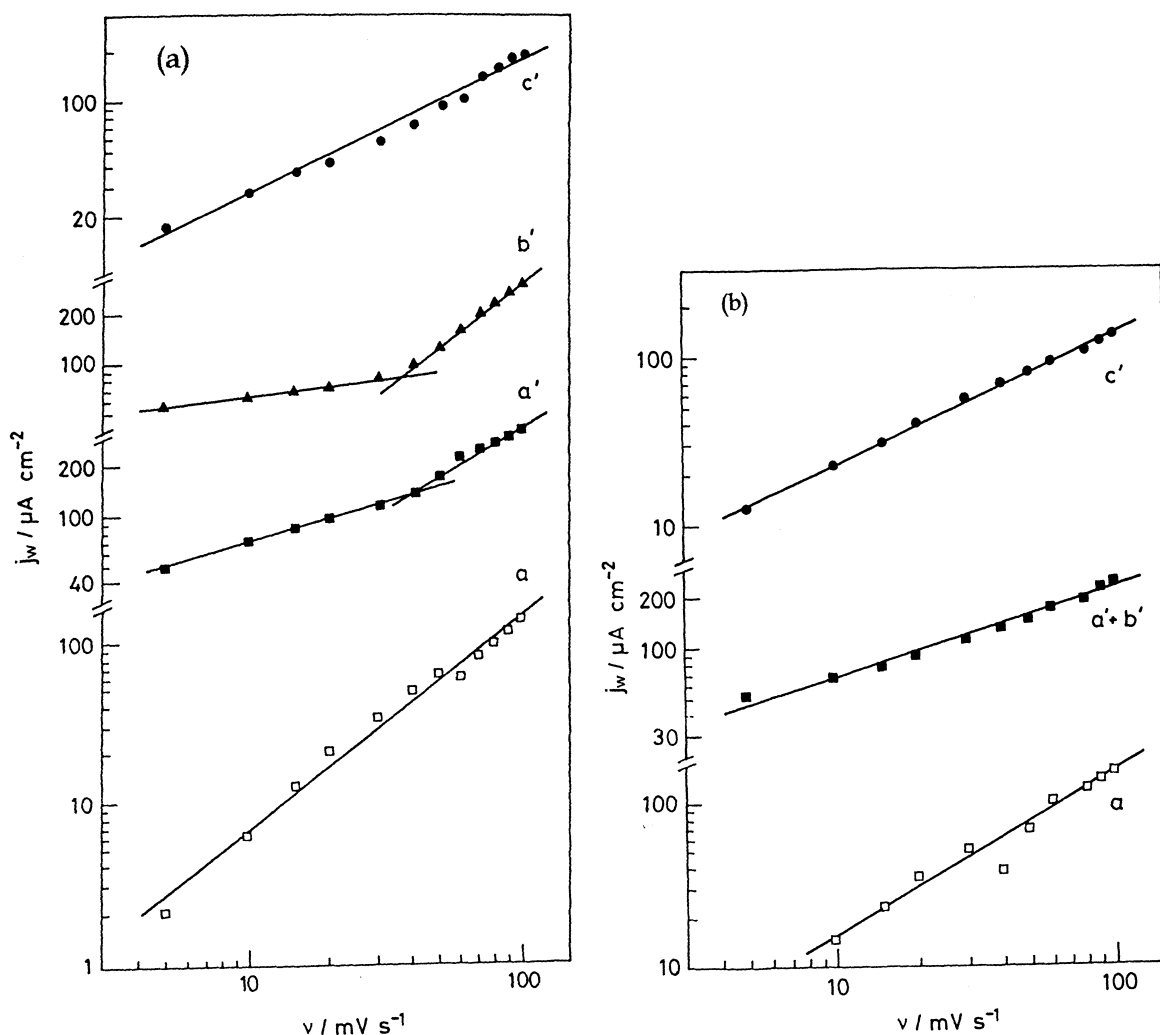

Fig. 8. Plots of log j_w against log v. (a) D films, waves: a ($\square$), a' ($\blacksquare$), b' ($\blacktriangle$) and c' ($\bullet$); (b) D' films, waves: a ($\square$), $a' + b'$ ($\blacksquare$) and c' ($\bullet$).

generated by a superficial capacitive oxidation mechanism at all scan rates, while the dopant anions exhibited high mobility [17]. In D films, the **a′** and **b′** reduction process (Figure 8(a)) showed a mixture of mechanisms. At $v < 50$ mV s^{-1} the slopes were close to 0.5; thus, this deinsertion process was diffusion controlled and the dopant anions had lower mobility. At $v > 50$ mV s^{-1} the slope values were close to 1, and the reduction process was controlled by charge transfer. The same mechanism occurred in the **c′** wave at all scan rates.

The dedoping process in D′ films tends to be diffusion controlled. The slopes of the **a′** + **b′** and **c′** waves were 0.5 ± 0.03 and 0.07 ± 0.02, respectively (Figure 8(b)).

The technological applications of conducting polymers related to electrochemical and electrochromic devices are well known. Combining the versatility of polymeric structure with successive charge-discharge processes, they could be used as clean batteries with high energy density. It is useful to inquire whether or not the electroactivity of the polymeric systems tends to decay upon prolonged operation of doping/dedoping cycles, probably due to the degradation of the polymeric deposits.

For this purpose, D′ films were subjected to continuous cycling in the potential range -1.4 and 2.3 V at $v = 30$ mV s^{-1}, for five days. Table 1 shows the total oxidation and reduction charge density (Q_{ox}^{T}, Q_{r}^{T}) as a function of the number of cycles (n). Generally, the polymer matrix was activated by cycling daily. Initially

the shape of the first cycle was not the same; however, after continuous treatment the polymer deposits were activated and the Q_{r}^{T}/Q_{ox}^{T} relationship tend to a constant value (Table 1).

In each experiment, the Q_{r}^{T} diminished with cycling but Q_{ox}^{T} increased, indicating that the polymeric material retained its capacity in the dopant insertion process but not in the deinsertion process.

During the fifth day the cathodic cycle showed some waves not previously identified, indicating structural changes in the polymeric matrix. The shape of the anodic cycle had changed.

4. Conclusions

The electropolymerization potential has a considerable influence on the electrochemical behaviour of polyfuran perchlorate doped films as it relates to their technological applications. That influence is confirmed by this study in that: (a) in cycling, when the positive potential at E_i constant was increased, D′ films exhibited deeper insertion/deinsertion of dopant anions, and therefore the values of the total charge densities (oxidation and reduction) were higher; (b) in cycling, when the negative potential limit was varied, reversible permeability of dopant anions was reached in D′ films at more negative potential values. The insulating state was attained later than in D films; (c) when the potential scan rate was modified, D′ films presented a superficial capacitive oxidation mechanism and a diffusion controlled mechanism in the dedoping processes. However, D films showed a mixture of mechanisms in the reduction processes depending on v; and (d) The polymeric material, D′ films, was submitted to continuous charge–discharge processes over successive days. Loss of electroactivity and degradation were confirmed.

Table 1. Total oxidation and reduction charge density (Q_{ox}^{T}, Q_{r}^{T}) and Q_{r}^{T}/Q_{ox}^{T} as a function of the number of cycles (n) during each day

n	Q_{ox}^{T} /mC cm^{-2}	Q_{r}^{T} /mC cm^{-2}	Q_{r}^{T}/Q_{ox}^{T}
1st day			
1	4.50	5.25	1.17
50	5.71	6.43	1.13
81	5.73	6.43	1.12
2nd day			
2	3.94	5.82	1.48
67	4.28	4.88	1.14
152	4.91	5.17	1.05
230	4.91	5.17	1.05
331	5.05	5.27	1.04
3rd day			
2	5.56	6.04	1.09
503	6.20	5.93	0.96
740	6.86	5.92	0.86
960	7.17	6.09	0.85
4th day			
2	5.44	4.88	0.90
21	4.28	4.58	1.07
116	5.04	4.81	0.95
167	5.22	4.93	0.94
340	5.21	5.14	0.99
5th day			
2	5.43	4.36	0.80
27	6.24	4.57	0.73
93	6.92	5.43	0.78
227	6.75	5.32	0.79

References

1. M.J. González-Tejera, I. Carrillo and I. Hernández-Fuentes, *Synth. Metals* **73** (1995) 135.
2. M.J. González-Tejera, I. Carrillo and I. Hernández-Fuentes, *Synth. Metals* **92** (1998) 187.
3. I. Carrillo, E. Sánchez de la Blanca, M.J. González-Tejera and I. Hernández-Fuentes, *Polymer* **42** (2001) 9447.
4. T.A. Skotheim, R.L. Elsenbaumer, J.R. Reynolds 'Handbook of Conducting Polymers' (Marcel Dekker, New York, 1998).
5. B. Demirboğa and A.M. Önal, *Synth. Metals*, **99** (1999) 237.
6. S. Glenis, M. Benz, E. Le Goff, J.L. Schindler, C.R. Kannewurf and M.G. Kanatzidis, *J. Am. Chem. Soc.* **115** (1993) 12519.
7. I. Carrillo, E. Sánchez de la Blanca, M.J. González-Tejera and I. Hernández-Fuentes, *Chem. Phys. Lett.* **229** (1994) 633.
8. E. Sánchez de la Blanca, I. Carrillo, M.J. González-Tejera and I. Hernández-Fuentes, *J. Polym. Sci. Part A* **38** (2000) 291.

9. T.F. Otero and C. Santamaría, *Synth. Metals* **51** (1992) 313.

10. D.A. Kaplin and S. Qutubuddin, *Polymer* **36** (1995) 1275.

11. M. Schirmeisen and F. Beck, *J. Appl. Electrochem.* **19** (1989) 401.

12. M.J. González-Tejera, I. Carrillo-Ramiro and I. Hernández-Fuentes, *Electrochim. Acta* **45** (2000) 1973.

13. R.A. Osteryoung, G. Lauer and F.C. Anson, *J. Electrochem. Soc.* **110** (1963) 926.

14. A. Bard and L.R. Faulkner, 'Electrochemical Methods. Fundamentals and Applications' (Wiley & Sons, New York, 1993).

15. C.H.A. Brett and A.M. Oliveira 'Electrochemistry Principles. Methods and Applications' (OUP, Oxford, UK, 1993).

16. E. Gileadi, E. Kirova-Eisner and J. Pencina, 'Interfacial Electrochemistry' (Addison-Wesley, MA, 1975).

17. T. Schimidzu, A. Ohtani, T. Iyoda and K. Honda, *J. Electroanal. Chem.* **224** (1987) 123.